# Mechanical properties of a model of attractive colloidal solutions

E. Zaccarelli,[1] G. Foffi,[1] K. A. Dawson,[1] F. Sciortino,[2] and P. Tartaglia[2]
[1]*Irish Centre for Colloid Science and Biomaterials, Department of Chemistry, University College Dublin, Belfield, Dublin 4, Ireland*
[2]*Dipartimento di Fisica, Università di Roma La Sapienza and Istituto Nazionale di Fisica della Materia, Unità di Roma La Sapienza, Piazzale Aldo Moro 2, 00185 Roma, Italy*
(Received 22 August 2000; published 23 February 2001)

We review the nature of glass transitions and the glasses arising from a square-well potential with a narrow and deep well. Our discussion is based on the mode coupling theory (MCT), and the predictions of glasses that we make refer to the ''ideal'' glasses predicted by this theory. We believe that the square-well system well represents colloidal particles with attractive interactions produced by grafted polymers, or depletion interactions. It has been recently shown that two types of glasses, an attractive and a repulsive one, are predicted by MCT for this model. The former can form at quite low densities. Most of our attention is directed at the mechanical properties of the glasses predicted by this theory. In particular we calculate the elastic shear modulus at zero frequency and the longitudinal stress modulus in the long wavelength limit. Results for both are presented along the glass-liquid transition curves and their interesting behavior is explained in terms of the underlying physics of the system.

DOI: 10.1103/PhysRevE.63.031501 PACS number(s): 61.25.Hq, 61.12.Ex, 82.70.Dd, 83.80.Hj

## I. INTRODUCTION

In recent years the idea that colloidal particles can form glassy structures has been established in a number of very interesting experimental and theoretical works. Most attention has been focused on colloidal particle systems that are dominated by repulsive interactions for which, at high packing fraction values, the glass represents an alternative packing to the usually more favorable crystal structure. These systems are well represented by a simple hard sphere model [1]. Where repulsive interactions dominate, the loss of ergodicity is lost due to blocking of the movements of particles by the quite dense surrounding cages formed by their nearest neighbors. In colloidal systems, mode coupling theory (MCT) [2] has played a leading role, interpreting and rationalizing some of the observations [3,4], and achieving quite acceptable numerical agreement in comparison to experiments [5–7].

Recently a new type of glass has arisen as the focus of interest [8–13]. This has been called the attractive glass. By attractive glass we imply that the loss of ergodicity is driven largely by strong short-ranged attractive interactions, in other words the ''stickiness'' of the particles to each other eventually dominates the thermal motions and the system freezes. Thus, close packing is no longer necessary for a glass to be stable and it transpires that such glasses can form at densities much lower than close packing.

Once having established the distinct nature of the attractive glass phenomenon, it is unsurprising that new phenomena should be associated with the system. For instance, MCT predicts that for well defined values of the temperature or packing fraction, the repulsive and attractive glasses differ only by their dynamical properties (as opposed to structural differences). Many questions remained unanswered in this arena and more research using different approaches must be developed before one has great confidence in the conclusions drawn so far. Nevertheless, the basic results emerging from MCT seem reasonable, and are reproducible, using a variety of different input static structure factors [13].

The situation in experimental studies is even less clear. It may be that colloidal glasses driven by attractive interactions have been observed and studied for some time, without clear recognition of their distinctive nature. Certainly some of the reported kinetically arrested states in colloidal systems, usually identified as ''gels,'' appear to arise at densities considerably lower than close packing [14–16]. Given that such observations appear to be associated with quite strong short-ranged attractions driven by depletion forces, or grafted chains onto larger particles, it would seem likely that indeed such systems are examples of those we currently discuss. On the other hand, as yet, there appear to be no clear reports of colloidal glass-glass transition in the experimental literature, but the typical logarithmic decay of density correlations that MCT predicts to happen close to an $A_3$ singularity [17] has been observed in the past for the glass transition of some polymeric systems [18,19]. More recently a logarithmic decay has been reported in a micellar system with short-ranged attractive interactions and this may be related to a proximate glass-glass transitions as these authors point out [20]. The clear recognition of two different glasses would be one clear and unambiguous signal that a distinctive attractive glassy state has been observed. Since this is expected to be an issue of considerable interest to experimentalists, it will be important to discuss those measurements that could differentiate the glasses, and this is one aim of the present work.

In this paper it is our intention to discuss the mechanical properties of the glasses formed when repulsive and attractive interactions are present, and where, under some conditions, the latter may become dominant. We shall work within the framework of the ideal MCT and present results for the linear elastic shear modulus at zero frequency, $G'(\omega=0)$, and for the longitudinal stress modulus in the hydrodynamic limit, corresponding to zero frequency and long wavelengths, $m_0$, to illustrate our point of view. The study of the elastic shear modulus has previously been addressed in [8], but a different potential is used there.

 

Our reasoning for presenting these results has two underlying strands of rationale. First, we have outlined the interesting features we believe to be present for colloidal systems where there are strong short-ranged potentials. However, we note that experiments in dense colloidal systems are far from simple and the number of techniques that can be reliably applied to examine these questions are much fewer than in dilute solutions due to multiple scattering and other limitations implied at high concentrations. Furthermore, when one works on the boundary between liquids and amorphous solids there are further restrictions in the options for experimental techniques that may be applied. In fact, the mechanical responses of an amorphous material are amongst the most simple and reliable methods of characterization. Even the bulk shear and longitudinal moduli are quite helpful in forming an initial assessment of the material itself, and of course they are themselves amongst the simplest parameters characterizing the transition from a liquid to a glass and, as we shall see, even between different glasses. Combined with this, it is clear that most practical applications of amorphous materials composed from colloidal particles will involve a strong interest in mechanical properties of the glass. Having said all this, the reader should be aware that many attractive glasses may be quite fragile and some thought will have to be applied in finding systems and methods where measurements can be made. In any case, these comments comprise the first strand of reasoning for our interest in the mechanical moduli of attractive glasses.

The second reason for our interest is quite different and involves a deeper analysis of the basis of the theory that we use to describe glassy systems. That is, rarely is MCT applied to a system simple enough that many issues can be worked out in detail but at the same time that there be a complete knowledge of the ''phase diagram'' and its dynamics. In our particular case, we shall study the square-well potential model with very short-ranged attractions. Some of the basic predictions for structure and dynamics of this model have been worked out in detail within the MCT formalism [13]. We have observed that the attractive glass introduces a new richness into the study and it naturally becomes of interest to understand what presumptions MCT is making about such phenomena. We shall be interested in such questions as, what part of the physics drives the attractive glass transition within MCT and whether this understanding can shed some light on the nature of the theory itself. Finally, as an aside we shall also seek to understand which physical characteristics of the colloidal particle and of the whole system sets the scale for the mechanical properties of a colloidal glass. Again, if MCT is correct, this will be of considerable practical interest.

In the light of these comments it is now possible to proceed to introduce the fundamental equations that define MCT and the mechanical responses that we calculate from it.

## II. THEORY

Mode coupling theory provides a description of the structural relaxation of super-cooled liquids. The variables of interest are the normalized density correlators defined as

$$\phi_q(t)=\langle \rho_{\mathbf{q}}^*(0)\rho_{\mathbf{q}}(t)\rangle/\langle|\rho_{\mathbf{q}}|^2\rangle \tag{1}$$

where $\rho_{\mathbf{q}}(t)=\Sigma_{j=1}^{N} e^{i\mathbf{q}\cdot\mathbf{r}_j(t)}$, with $N$ being the number of particles in the system. By using the Mori-Zwanzig formalism, it can be shown [2] that the equations of motion for the variables $\phi_q(t)$ are,

$$\ddot{\phi}_q(t)+\Omega_q^2\phi_q(t)+\nu_q\dot{\phi}_q(t)+\Omega_q^2\int_0^t m_q(t-t')\dot{\phi}_q(t')dt'=0 \tag{2}$$

for Newtonian dynamics. The two quantities $\Omega_q$ and $\nu_q$ are respectively the characteristic frequency of the phonon-type motions of the fluid and a term that describes instantaneous damping, the latter arising from the ''fast'' contribution to the memory function. They are defined as

$$\Omega_q=\frac{q^2k_BT}{mS(q)}, \tag{3}$$

$$\nu_q=\nu_1q^2 \tag{4}$$

and typically one chooses $\nu_1=1$ in the calculations. Equation (2) is formally exact for a set of $N$ particles.

To describe the dynamics of colloidal suspensions, they have been modified neglecting the inertia term and including the solvent contributions [21]. Thus, we have

$$\tilde{\phi}_q(t)+q^2D_q^s\left\{\phi_q(t)+\int_0^t m_q(t-t')\tilde{\phi}_q(t')dt'\right\}=0 \tag{5}$$

where $D_q^s$ is the Brownian short-time diffusion.

The crucial approximation of MCT consists of giving an explicit factorized form for the memory kernel in Eqs. (2) and (5) as

$$m_q=\frac{1}{2}\int\frac{d^3k}{(2\pi)^3}V(\mathbf{q},\mathbf{k})\phi_k(t)\phi_{|\mathbf{q}-\mathbf{k}|}(t) \tag{6}$$

and the vertex functions are the coupling constants of the theory,

$$V(\mathbf{q},\mathbf{k})=\frac{\rho}{q^4}\{\mathbf{q}\cdot(\mathbf{q}-\mathbf{k})c_{|\mathbf{q}-\mathbf{k}|}+\mathbf{q}\cdot\mathbf{k}c_k\}^2S_qS_kS_{|\mathbf{q}-\mathbf{k}|}. \tag{7}$$

In the static limit $t\to\infty$, independently on the type of microscopic dynamics, the density correlators $\phi_q(t)$ tend to a finite value $f_q=\langle\rho_q^*(0)\rho_q(\infty)\rangle/\langle|\rho_q(0)|^2\rangle$, known as the nonergodicity factor, if the system is kinetically arrested. This loss of ergodicity for the density correlators is seen as the transition to a kinetic glassy state within MCT. Thus, Eq. (2) becomes in the static limit,

$$\frac{f_q}{1-f_q}=\frac{1}{2}\int\frac{d^3k}{(2\pi)^3}V(\mathbf{q},\mathbf{k})f_kf_{|\mathbf{q}-\mathbf{k}|}. \tag{8}$$

It is clear that $f_q=0$ always corresponds to a solution of Eq. (8). This corresponds to an ergodic state of the system in which the correlations decay for long times. For some criti-

cal values of the thermodynamic parameters (control parameters), such as temperature and density, there appear bifurcations of the solutions of Eq. (8), that produce nonzero solutions. These correspond to the nonergodic states of the system, and given that there is no positional order in the system we identify these solutions as glasses. The bifurcations can be multiple, up to the number of control parameters of the system. Thus, when a bifurcation gives rise to more than two solutions of Eq. (8), there will exist multiple solutions with finite nonergodicity factors. In this case, MCT predicts that only the state corresponding to the largest value of $f_q$ is the long-time limit solution of the equation [2,22].

With an input structure factor, we can now solve the MCT equations for the nonergodicity parameter, and it is possible to calculate the ''phase diagram'' of the system, localizing the regions in the thermodynamic parameter space where the system is in the fluid ($f_q=0$) or in the glassy state ($f_q>0$) and also some mechanical properties of the glass itself. Note that by ''phase diagram'' we mean here that the fluid and glassy states of the system are identified, the latter being nonequilibrium states of matter.

A particularly interesting physical quantity is the elastic shear modulus $G'(\omega)$. From the shear viscosity for a colloidal system [3,23], it is possible to evaluate the elastic shear modulus within the MCT approximation in the limit $\omega\to 0$ to give [8]

$$G'(\phi,T)=\frac{d^3}{60\pi^2}\int_0^\infty dk k^4\left(\frac{d\ln S_k}{dk}f_k\right)^2, \tag{9}$$

where $G'$ is in units of $(k_BT)/d^3$, where $T$ is the temperature of the system and $d$ is the diameter of a particle.

Another property that can be examined by experimentalists is the longitudinal stress modulus $m_0$. We will discuss only the hydrodynamic approximation of this quantity [3,24], that is easily obtained taking the limits $q\to 0$ and $t\to\infty$ in Eqs. (6) and (7), giving that

$$m_{q=0}(\omega=0)=m_0=\int_0^\infty V_k f_k^2 dk, \tag{10}$$

where the long wavelength limit of the vertex function is given by

$$V_k=\rho S_{q=0}\left(\frac{S_k k}{2\pi}\right)^2\left[c_k^2+\frac{2}{3}\left(k\frac{\partial c_k}{\partial k}\right)c_k+\frac{1}{5}\left(k\frac{\partial c_k}{\partial k}\right)^2\right]. \tag{11}$$

It is possible to relate $m_0$ to the velocity of sound in glass (solid) compared to that in liquid at the transition line. Thus, we observe that the speed of sound in a liquid is given in terms of the compressibility of the liquid whilst the formation of a solid leads to a finite memory kernel at long times and consequently an increment $m_0$,

$$\frac{v_\infty}{v_0}=\sqrt{1+m_0}\,, \tag{12}$$

where $v_0$ and $v_\infty$ are, respectively, the limiting low- and high-frequency sound speeds.

Since the longitudinal modulus is a close equivalent of the shear modulus, but for extensional distortions, it is natural that we should seek to calculate and compare the two quantities. We would like to point out to experimentalists who may be interested in this field that the theory as applied to ratios of quantities at the transition may be quite well modeled by the theory and less dependent on model details. We therefore recommend some thought on how experiments of this type might be carried out.

We have solved [13] the MCT equations for the ideal glass-transitions (8) for a system of monodisperse colloidal particles, interacting via a square well potential, with a very narrow-range attractive well, defined as

$$V(r)=\begin{cases}\infty, & r<d\\ -\beta u_0, & d<r<d+\Delta\\ 0, & d+\Delta<r\end{cases} \tag{13}$$

where $\beta=(k_BT)^{-1}$ with $k_B$ the Boltzmann's constant and $\Delta$ is the well width, which can be related to the small parameter $\epsilon=\Delta/(d+\Delta)$.

To calculate numerically the equilibrium structure factors $S(q)$ of such a system, one can use the mean-spherical approximation (MSA), Percus-Yevick, or other closure relations for the Ornstein-Zernike integral equation [13]. Reference [13] compares many of the important features of the statics and dynamics of these systems using MSA and Percus-Yevick (PY) approximations. In view of the good agreements found between these closures, we shall here present only calculations based on the PY closure. The phase diagram for different values of the well-width of the potential has been presented in Ref. [13]. In particular, for the mechanical results, we will focus our attention on the case where $\epsilon=0.03$. Here we report in Fig. 1 more details and present both the glass transitions as well as the liquid-gas spinodal, which may be regarded as an approximation to the equilibrium phase diagram. This provides the reader with an overview of where we expect to find all the phenomena discussed later. Thus, in Fig. 1 we can see the curves labeled, respectively, $B_1$ representing the fluid-repulsive glass and $B_2$ representing the fluid-attractive glass transition. In the inset, we have shown in more detail the attractive-repulsive glass transition curve with its end-point labeled as $A_3$. Beyond this point, the two types of glasses become indistinguishable. Also, the dashed curve in the low volume fraction region represents the gas-liquid spinodal calculated via an expansion in $\epsilon$ around the Baxter potential [25,26] and in good agreement with numerical calculations for the square-well potential, at least to the right-hand side of the critical point (larger volume fractions). We comment here that the left-hand side branch of the spinodal is singular for a Baxter model because it corresponds to complex values of the characteristic parameters $\lambda$, and also for such low packing fractions and temperatures the numerical PY solution of the square-well potential was not reliable. Thus, the only true meaningful branch of the spinodal in Fig. 1 is the ''liquid''

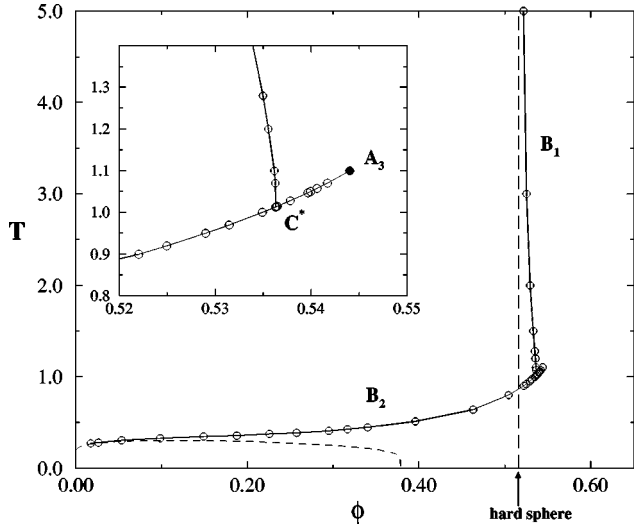


FIG. 1. Phase diagram of a colloidal system interacting via a square-well potential, defined as in Eq. (13) with $\epsilon=0.03$, solved within Percus-Yevick closure relation and calculated by solving the MCT equation (8). The horizontal axis represents the colloid volume fraction $\phi$ and the vertical axis the temperature in units of $K_B/u_0$. The curve labeled as $B_1$ represents the fluid-repulsive glass transition that is in agreement with the hard-sphere limit for MCT at large temperatures (vertical dashed line at $\phi\simeq 0.516$). The curve $B_2$ represents the fluid-attractive glass transition. In the inset, it is shown in more detail the attractive-repulsive glass transition curve with its endpoint labeled as $A_3$. Also, the dashed curve in the low volume fraction region represents the gas-liquid spinodal.

branch that corresponds approximately to $\phi \geqslant 0.14$, where we estimated that the critical point is located corresponding to a critical temperature of approximately 0.3.

It is interesting to note that while the curve $B_1$ is almost vertical, $B_2$ is largely horizontal and the two meet forming a nonzero angle. The fact that the repulsive glass-liquid transition curve is vertical is ensured by the fact that classification is driven only by the hard core, which lacks any energy scale. On the contrary, the attractive glass-liquid one, being fairly horizontal, implies that there is a single well-characterized energy scale that drives the glassification.

## III. RESULTS

To discuss our results we shall frequently refer to the phase diagram in Fig. 1. Let us begin by looking at what is at first sight one of the more striking predictions of the calculations, the transition between two types of glasses and their merging at an endpoint that has been labeled as the $A_3$ point [2], since it represents a third-order singularity of the MCT equation (8).

The reader should be aware that, within MCT, on the transition lines, whether they be liquid-glass or glass-glass, the two states of matter do not have any difference in density or in structure and are differentiated in terms of the nonergodicity factors $f_q$. Since this is a nonequilibrium property of the system, we note that there is essentially no equilibrium quantity that establishes the difference in phases and the order parameter must therefore be composed of $f_q$.

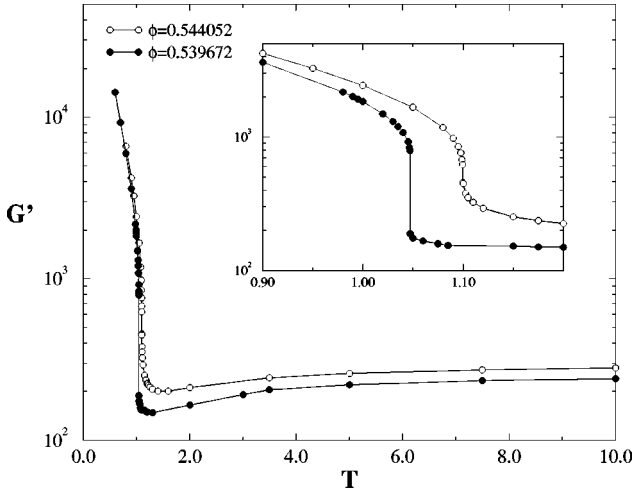


FIG. 2. Plot of the elastic shear modulus $G'$ as a function of temperature for $\phi=0.539\,672$ (black circles) and $\phi=0.544\,052$ (white circles). The first value corresponds to crossing the glass-glass critical line, while the second corresponds nearly to the endpoint $A_3$ of this line.

Since the repulsive glass and the attractive glass illustrated in Fig. 1 and inset to that figure are differentiated only by the changes of their $f_q$, it is therefore natural to ask what differences are implied in the shear modulus and other mechanical properties of these two glasses, and how these differences vanish as we approach the endpoint where the two glasses become identical. We have examined this question for the example of the shear modulus.

Thus, in Fig. 2 we plot $G'$ as a function of increasing temperature for two fixed volume fractions $\phi=0.539\,672$ and $\phi=0.544\,052$, both of them involving a crossing of the glass-glass transition curve. For the smaller of these two volume fractions, it is evident from the figure that upon crossing the transition, there appears a sharp discontinuity in the shear modulus. For the larger one, which is very close to the endpoint value packing fraction $\phi_{A_3}$ crossing the curve, there is negligible difference between the shear moduli of the two glasses. Evidently, it is of interest to define $\Delta G'$, the difference in $G'$ found in the two glasses at the transition and to examine this as a function of $\Delta\phi$ and $\Delta T$, respectively, the differences in volume fraction and temperature from their endpoint values, which we evaluated as $\phi_{A_3}\simeq 0.5441$ and $T_{A_3}\simeq 1.099\,75$. We numerically find, over the whole range of the glass-glass transition, that the laws connecting these two quantities are

$$\Delta G' \sim (\Delta\phi)^p, \quad \Delta\phi=\phi-\phi_{A_3}, \tag{14}$$

$$\Delta G' \sim (\Delta T)^q, \quad \Delta T=T-T_{A_3}, \tag{15}$$

where $p$ is approximately $0.33\pm 0.03$ and $q$ is approximately $0.32\pm 0.08$. The errors in these estimates could be reduced with larger computational effort, but there do indeed appear to be power laws to high precision. These exponents can be explained by a simple argument. We know that near an $A_2$

singularity $f_q$ is a solution of a second-order polynomial, while near an $A_3$ point it is solution of a cubic one. This implies

$$f_q - f_q^{A_2} \sim (\epsilon_{A_2})^{1/2}, \tag{16}$$

$$f_q - f_q^{A_3} \sim (\epsilon_{A_3})^{1/3}, \tag{17}$$

where $\epsilon_{A_i}$ can be both $T - T_{A_i}$ or $\phi - \phi_{A_i}$. Thus, evaluating the expression (9) for $G'$ in the proximity of the singularity $A_3$ gives, in the leading order, an exponent 1/3.

It will be of interest for experimentalists to seek the proposed phenomenon of glass-glass transition and to deduce estimates of any exponents that arise. Amongst the most accessible of these is that of the shear modulus discussed above. However, we do note the reservation that it is likely that there is some associated structural and density relaxation at the glass-glass transition and this may disturb the simple power law outlined above.

Evidently, a fairly practical comment that emerges from these results is that the repulsive glass stiffness with respect to shear is much smaller than the attractive glass one as indicated by the large vertical discontinuity shown in the inset of Fig. 1. This reflects the fact that particles in the attractive glass are bonded by the stickiness of the potential, whilst in the repulsive one there is no real bonding between them, thus implying that they are more easily broken apart under shear. Also, as expected, the attractive glass shear modulus increases considerably with the decrease of temperature, the attractions between particles becoming more relevant, whilst for the repulsive glass there are no significant changes with temperature, there being no energy scale involved in its formation.

Having outlined our results for the shear modulus differences between the two glasses, it is perhaps worthwhile to revisit the physical meaning and implications of these results. First, all the differences in mechanical properties here come from the nonergodicity factor alone rather than static structure since the two states have the same structure factor that is essentially the structure factor of the liquid to which the MCT glass is referred. It is, therefore, interesting to note that the differences in $f_q$'s between the two types of glass, reflecting as they do the nature and efficiency of the relaxation processes at different length scales, lead to such large differences in moduli.

Let us now turn to another part of the phase diagram of these systems. We have earlier alluded to the work by Verduin and Dhont [14] for a very short-ranged attractive colloidal system where they found some nonergodic states at low temperature. These they interpreted as gel states but in line with the ideas laid out in this paper they might also be viewed as attractive glasses as it was already discussed in [8]. In fact, the horizontal portion of the glass-liquid curve in their phase diagram already is indicative that the energy scale is playing a leading role rather than packing forces. Therefore, we believe that it will transpire that it is quite feasible to prepare and study attractive glasses in some detail.

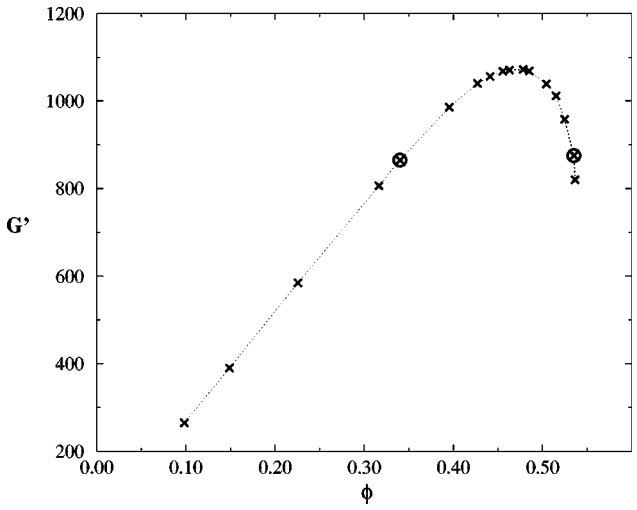


FIG. 3. Plot of the elastic shear modulus $G'$ of an attractive glass as a function of the volume fraction $\phi$ along the liquid-glass transition corresponding to packing fraction values up to $\phi \simeq 0.535$ (as in Fig. 1). We note that the predicted value of the volume fraction for hard spheres to undergo a glass transition is $\phi_{HS} \simeq 0.52$. However, the decrease of the magnitude of the shear modulus starts before we reach this value, at approximately $\phi \simeq 0.48$. This corresponds to the stiffest glass we can produce along the transition curve.

In particular, it will be possible to study many properties along the liquid-glass transition. We comment first that any attempts to design colloidal particles with the appropriate well shape will most likely involve some uncertainties. Thus, the obvious methods of coating the spheres with some attractive layer or using depletion forces in polymer solutions cannot hope to exactly reproduce the parameters and shape of the square well. Therefore, the curve of liquid-glass transitions corresponding to the square well may be fit to experimental data. Though it may not be correct in all details, it should be reasonably accurate in its behavior as a function of packing fraction of spheres and in reproducing many of the attendant phenomena. Thus, irrespective of the extent of agreement between the square-well potential and the effective potential that is ultimately tested in experiments, we may be fairly certain that some predictions of our theory will be more robust than others. Amongst these we might again include the typical evolution of the mechanical properties as a function of packing fraction.

Therefore, it becomes of some interest to construct the evolution of $G'$ on the glass side of the liquid-glass transition across an extensive range of packing fractions encompassing all of what would be viewed as the attractive glass, to be able to compare these results with experiments. Thus, in Fig. 3 we present the curve of $G'$ as a function of $\phi$ along the attractive glass line, labeled $B_2$ in Fig. 1. We note that this curve extends to quite low volume fractions and that it is linear in a large range of volume fractions. In fact this is true for all those values of $\phi$ where the attractive interactions are considered to be completely dominant. Ultimately the curve turns downwards towards typical repulsive glass values of $G'$ when we go to higher volume fraction. Even so, we

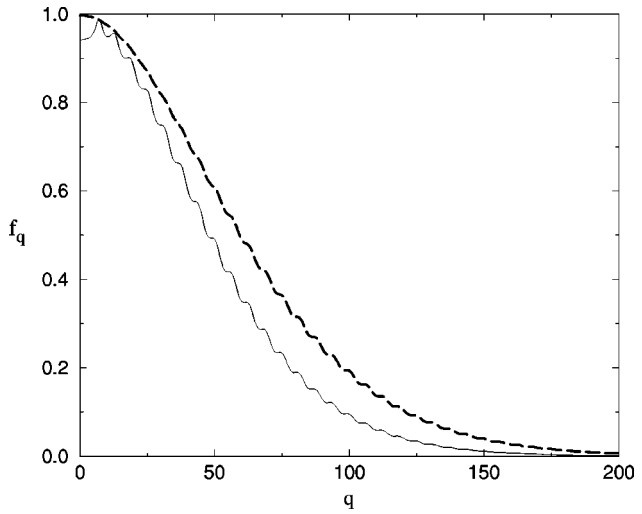


FIG. 4. Nonergodicity factors at the glass transition corresponding to the circled points in Fig. 3 where $q$ is expressed in units of particle radius ($r=1$). The full line represents the nonergodicity factor on the repulsive side and the long dashed line represents the state on the attractive side. The nonergodicity factors are certainly different, but it is of interest to consider Fig. 6 where we learn that these difference in nonergodicity factor alone is sufficient to cause the considerable softening of the glass as the volume fraction exceeds its critical value of $\phi \simeq 0.48$.

might have expected that the downward bending of the curve would have happened very close to the critical hard sphere packing fraction, $\phi \simeq 0.52$, whereas it commences around $\phi \simeq 0.485$. Very similar characteristics for the shear modulus along the attractive glass transition line have also been found for the attractive Yukawa potential [8].

Finally as a matter of curiosity let us draw attention to one aspect of the shear modulus plot in Fig. 3. Consider the two circled points on the curve in Fig. 3. They correspond to states having approximately the same shear modulus but quite different packing fractions, i.e., $\phi_1 \simeq 0.34$ and $\phi_2 \simeq 0.535$. Thus, we represent in Fig. 4 the respective nonergodicity parameters of the two states for comparison. It is interesting to note that whilst the range of the two is almost the same as it should be since they both represent states of attractive glass, the one corresponding to the lower packing fraction exhibits a more pronounced nonergodicity of the system at every length scale. The fact that we have the same shear modulus is a reflection that both the nonergodicity and static structure factors are relevant for the modulus and in this case we see that they compensate each other so that we can ''build,'' from the same system two glasses with the same stiffness with respect to shear, but having completely different packings and different structure. This would be an interesting phenomenon if confirmed by experiments.

Now it is worth considering the MCT prediction that glasses can exist at volume fractions less than 10% as indicated in the phase diagram, Fig. 1. Certainly attractive glasses can and should form at much lower fractions than repulsive glasses but we must not accept the results of MCT blindly. Note carefully the limitation that MCT does not permit the self-consistent relaxation of structure in the glass phase and consequently the density cannot adapt to the new situation as the ergodicity is lost. The consequences of this have been outlined for the glass-glass transition but one should be aware also for the possibility for qualitatively mistaken predictions in the region of a liquid-glass transition where there is a metastable liquid-gas phase separation as in Fig. 1. Thus we must acknowledge the tendency for separation into more and less dense phases that could be superimposed on the liquid-glass transition curve $B_1$. That this does occur has not been proved but if it did, our MCT calculation would not accommodate it.

Given this concern, we have calculated the mean number of bonded spheres $n_b$ to a central sphere at the formation of the attractive glass along the curve $B_2$. We consider as sufficient condition for bonding that the distance between two particles is up to the attractive well width. Thus, it is easy to estimate $n_b$ by carrying out the integration over the pair-correlation function such that only those spheres falling within the attractive well are included in the integration. From the definition of the potential (13), we then have

$$n_b = \int_0^{(d+\Delta)} \rho g(r) d\mathbf{r}. \tag{18}$$

For convenience we also calculated one estimate of the mean coordination number $n_c$ around a sphere irrespective of whether the spheres are bonded or not.

Nevertheless, we have

$$n_c = \int_0^{r^*} \rho g(r) d\mathbf{r}, \tag{19}$$

where $r^*$ corresponds to our estimation of the first peak of the pair-correlation function $g(r)$.

The mean bonding number is a well-defined quantity and is calculated exactly here, whereas the mean coordination number is not so well defined. The former may be relied on, the latter is used only as a comparison to the mean bonding number.

Both results are plotted in Fig. 5 as a function of the volume fraction along the curve $B_2$. It is striking that both curves are nearly linear. However, the interesting thing to note is that the mean bonding number at $\phi \simeq 0.10$ is around 1.5. Also, we can roughly estimate that only at $\phi \simeq 0.17$ we find $n_b \simeq 2$. Thus, it seems unlikely that extended mechanically stable structures can exist for such small bonding numbers. Indeed, a mean bonding number of 2 would imply polymeric structures and for bonding numbers a bit larger than 2 we may have enough cross-links to establish a network and finite shear moduli. Just how large the mean bonding number has to be before a finite shear modulus is obtained, we cannot say. Very simple arguments based on counting degrees of rotational and vibrational freedom, and requiring that there be no zero modes of the energy indicate that the minimum number of bonds to form an extended structure for a chemical glass should be about 2.4 [27]. However these arguments have not been shown to be relevant to the present case, so there is little more progress that can be made now.

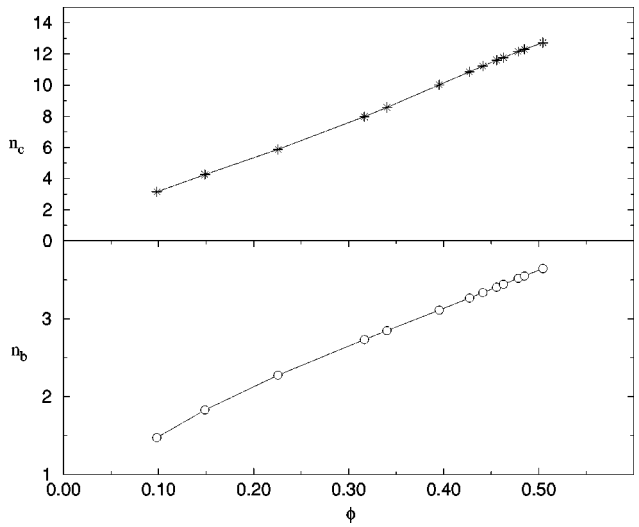


FIG. 5. Plots of the coordination number $n_c$ (19) and the mean bonding number $n_b$ (18) as a function of the volume fraction $\phi$ along the liquid-attractive glass transition line $B_2$. The two behaviors are nearly linear, except for small deviations, at low volume fraction for $n_b$. As discussed in the text, in this region where $n_b$ is less than 2, we question the existence of the attractive glass as predicted by MCT because there are not enough bonds between the particles to allow the formation of a rigid structure.

The discussion should, however, alert the reader to the possibility that somewhere along the $B_1$ line, possibly when the bonding number is a little less than 2, the reduction of any further bonds in the system might cause it to decompose, presumably into a less dense and a more dense phase. These remain open questions for the moment but as MCT becomes applied more to glasses driven by attractions, it will be important to consider them in future.

Of course, another fundamental question that should be addressed in future is the applicability of idealized MCT to colloidal systems with attractive interactions. Indeed, whilst for hard-sphere-type systems the idealized theory has been found in good agreement with experimental results, it is not yet clear whether for attractive systems, at lower densities, activated processes may become important so that hopping should be included in the theory for a better description of this type of systems. Our present opinion is that the idealized theory is likely to be useful for moderate densities where the bonding number is somewhat larger than 2. We do not preclude the possibility that for much lower densities, the theory may still be suggestive, and indeed there have been already attempts to interpret these regimes [8,10,11].

Thus, all this discussion leads us to seek a somewhat deeper understanding of exactly what the basis of the mode coupling predictions are. By this we mean, we seek to understand the essential features of the theory as it relates to attractive glasses. One of the points that we would like to probe a little more is to understand just how local MCT is in its understanding of the loss of ergodicity, and in its estimates of the main features of mechanical moduli. The simplest possible proposition would be that essentially with knowledge of the number of bonds and strength of associations between nearest neighbor particles, we would estimate a correct MCT transition and perhaps, even estimate a correct mechanical response. We now seek to test this hypothesis. We shall examine this question in two steps beginning with the calculation of the nonergodicity factor that determines the glass transition itself, then progressing to the shear modulus.

For simplicity, we call $q^*$ the wave vector corresponding to the first peak of the structure factor. We then proceeded recalculating the liquid-glass transition using two approximations. First, we used the correct short-wavelength behavior of the structure factor for $(q>q^*)$, in solving the MCT equations (8) but using for the long-wavelength part of the structure factor (i.e., $q<q^*$) the corresponding part of it for a packing fraction that we chose arbitrarily. We considered both $\phi\simeq 0.31$ and $\phi\simeq 0.39$ obtaining no significant changes in the results. We found that the essential features of the trends and quantitative evolution of the transition are set only by the short-ranged part of the structure factor, then irrespective of what we chose for the long-wavelength part of it. Thus, length scales involving only the hard core and attractive well of a spherical particle are sufficient to determine the glass-liquid transition within MCT. Indeed, we investigated a few points along the curve $B_2$ and we also found that the transition temperatures are reproduced within a few percents error.

To confirm these results, we also tried to evaluate the curve $B_2$ using an opposite strategy. We then used the correct long-wavelength part of the structure factor $(q<q^*)$ and as short-ranged part, the corresponding part for the same values of packing fractions as before. This leads not only to much larger errors in the glass-liquid curve $B_2$, but what is more important, to the wrong evolution of that curve with volume fraction; this means that the curve was not only shifted but also changed in its shape. We may therefore conclude that whatever the full content of MCT, one can estimate the location of the transition curve of the attractive glass to high precision by knowing only local information about the particles around a central particle. Long-ranged effects, therefore appear not to play a central role in this aspect of the MCT description. The same observation had been made earlier for the Yukawa model and for the square-well potential, both solved within MSA [8,13]. Thus, this is a general feature of the theory itself, independent on the model or the approximation chosen to solve it.

We now turn to another natural question about the predictions of MCT. After having analyzed what the dominant contributions are for the prediction of the location of the glass transition, we want to investigate what is important in the determination of the mechanical properties of the glass within the theory. To do so, we still refer to the results of the shear modulus $G'$ in Fig. 3.

Thus, we note that in Eq. (9), there are evidently two important contributions to the shear modulus, the nonergodicity factor and the logarithmic derivative of the structure factor. We may ask if only one of these features provides the main contribution to the shear modulus. To check this we may proceed as before, first retaining the correct structure factor and using the nonergodicity factor of a chosen value of packing fraction $(\phi=0.39)$, and then vice versa. The

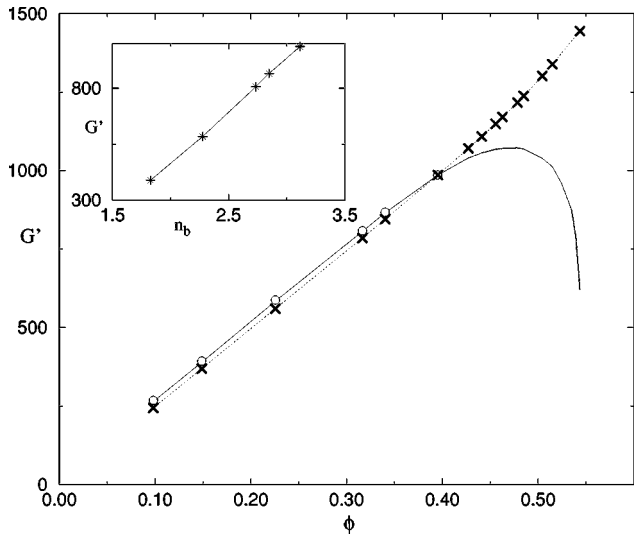


FIG. 6. Plot of the elastic shear modulus $G'$ as a function of $\phi$, as in Fig. 3 (full line). Superimposed we have plotted $G'$ calculated by using an incorrect reference $f_q$ (see text) and the correct structure factor (crosses). Results obtained by using the correct nonergodicity factor and only the exact short length-scale contribution for $S(q)$ have been plotted using circles. Together these approximate curves indicate that for most of the range of stability of the attractive glasses its properties are dominated by the short length scale of the structure factor. Also, providing the system is nonergodic ($f_q > 0$), the degree to which it is so is not a very important parameter in determining the mechanical properties we discuss. However, at higher densities the shear rigidity of the glass begins to decrease again as we approach a repulsive glass. This behavior cannot be described as above, and we now need to use the correct nonergodic factor, and the details of the structure factor now becomes less relevant in determining shear rigidity. Inset: Plot of the elastic shear modulus versus the number of bond $n_b$, showing an almost linear dependence. Here we see that for the true attractive glass the shear rigidity is close to bring linearly dependent on the number of nearest neighbors within the range of attraction.

question may be further refined by asking whether it is possible to further locate the main driving force of the shear modulus as being short ($q > q^*$) or long ($q < q^*$) length scales.

The answer is striking. With almost quantitative accuracy we find that the linear behavior of the shear modulus with volume fraction, in the purely attractive region, which we can define being in the range of volume fractions between 0.17 and 0.4 originates solely in the short length-scale ($q > q^*$) behavior of the structure factor as shown in Fig. 6. We represent here the curve, already reported in Fig. 3, with superimposed data obtained by using the chosen $f_q$ and the true structure factor (crosses) and those obtained by using the true nonergodicity factor and only the exact short length-scale contribution for $S(q)$ (circles). Thus, providing the nonergodicity factor is finite and on the correct scale, the shear modulus is relatively insensitive across the whole attractive glass region to its details, being only shifted by a small amount. We note that in the figure all the sets of data are coincident at $\phi = 0.39$ since this is the chosen value of reference for the different cases. Since we find, as before, that only the short length-scale picture of the system is really involved in the determination of $G'$ (circles), we can explain the linear behavior of the shear modulus with packing fraction in the attractive region, being directly related to the number of bondings. Thus, we represent $G'$ in function of $n_b$ in the inset of Fig. 6 and we show that there also exists a linear relation between them.

Finally, we turn to analyze what happens for the phenomenology of the shear modulus at higher packing fractions, beyond what we believe is the pure attractive region, where $G'$ undergoes a rather rapid decline. We have pointed out already that along the glass-liquid curve in Fig. 3 this rapid decrease of the shear modulus happens as we approach $\phi \simeq 0.48$, which is a value quite below the close-packed structure appropriate for the hard core. It may be argued that this phenomenon is hardly surprising since we know that finally, the shear modulus must decrease to values characteristic of a repulsive glass. These are much smaller since, as we have earlier pointed out, there are no attractive interactions and no effectively bonded particles to the central one. However, it is nevertheless interesting to understand why the shear modulus softens quite dramatically at that particular packing fraction and by what means the effective attractions are being screened in the system in this region of densities.

To understand this point, we have studied the thermodynamic pressure for a square-well potential, given in Ref. [28]. In particular, we have examined the pressure and compressibility of the liquid along the glass-liquid curve in order to exclude the possibility that there be any anomalies in the liquid itself in the relevant region. We found no anomalies within the PY approximation in the region of packings from approximately 0.45 up to beyond the endpoint value $\phi_{A_3}$. It is then interesting to note that whilst the liquid is perfectly normal, the proximate glass undergoes this softening at well-defined values of $\phi$ and $T$ corresponding to the decrease of the shear modulus. In essence we find that the softening of the glass, whilst it certainly originates in cancellations between hard core and attractive parts of the potential as the density increases, occurs mechanistically within the MCT memory kernel.

To be more precise, we have used the same strategy as in the purely attractive region to examine the different contributions of the structure factor and of the nonergodicity factor to the shear modulus. So, in Fig. 6 the data represented with crosses, corresponding to the correct structure factor and a fixed arbitrary nonergodicity factor, are also represented at higher volume fractions. It is evident that their linear behavior, entirely due to the structure factor, persists with increasing density. Conversely, by a similar analysis, where the structure factor was chosen arbitrarily and the nonergodicity factor was the correct one, we have found that the principal origin of the decrease in the modulus is the change in the nonergodicity factor since in this region it is changing from a characteristic attractive to a repulsive form. The smaller integral resulting in Eq. (9) reflects the fact that the attractive glass is less mobile due to the formation of attractive bonds. Thus, it can only be the nonergodicity factor, solution of the MCT equation (8), which is responsible for the softening of the glass.

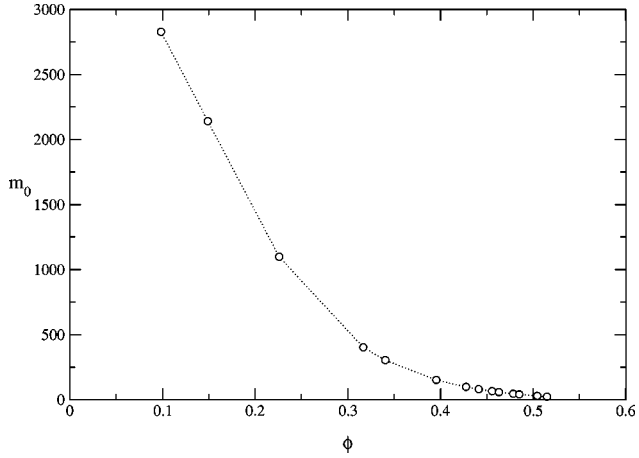


FIG. 7. Longitudinal stress modulus $m_0$ as a function of the packing fraction $\phi$ along the part of the curve labeled $B_2$ in Fig. 1 corresponding to the transition between an attractive glass and a liquid.

We now turn our attention to the behavior of the longitudinal stress modulus. We have already shown that it presents a discontinuous behavior, similar to the elastic shear modulus, upon crossing the glass-glass transition in [13]. Now we show $m_0$ along the curve $B_2$, i.e., along the attractive glass-liquid transition line in Fig. 7, on the glass side of the transition in the same way as we did for the shear modulus. We conclude that for increasing packing fraction, though the glass becomes more rigid with respect to shear, reaching a maximum at $\phi \simeq 0.48$, the longitudinal modulus decreases continuously along that same curve coming close to its characteristic liquid value very close to the point where the two curves $B_1$ and $B_2$ meet, corresponding approximately to $\phi \simeq 0.536$. At first sight this seems counter-intuitive since we expect that the extensional rigidity should increase with density, at least up to that density where the elastic shear constantly increases.

If we examine the longitudinal modulus as a function of density, for temperatures that cause the system to be within the repulsive-glass region only, the normal expectation of increased longitudinal modulus with increasing density is confirmed as illustrated in Fig. 8(a). In Fig. 8(b), instead, we have the opposite behavior of the longitudinal modulus with density for a much lower temperature than in Fig. 8(a). Indeed, from Eq. (10), it is clear that the modulus depends on the zero-momentum limit of the structure factor, appearing as a prefactor, and the data correspond to a temperature for which the system passes very closely to the critical point or spinodal curve of the underlying liquid-gas transition. In fact, MCT implies that the long length-scale associated with the proximate liquid, when it is near a critical point, or otherwise the underlying spinodal is quenched into the solid glass because both liquid and glass have the same structure factor. Within MCT the large modulus in the attractive glass region therefore derives essentially from this large quenched correlation length in the glass rather than any microscopic interaction. We note that there is no such quenched long length-scale dependence implied by the shear modulus either in the formula (9) or from the results showed in Figs. 3 and 6. In fact, as we showed earlier, the shear modulus in the attractive region is mainly determined by nearest neighbor adhesions. The striking difference in the behaviors of the two modulii is an interesting prediction of MCT when applied to attractive glasses. Possibly some of this variation originates because long length-scale structures are quenched into the glass. Whilst we do not know if it is true in nature, the strong distinction between longitudinal modulus and shear modulus along the liquid-glass curve will be readily testable in experiments on colloidal systems.

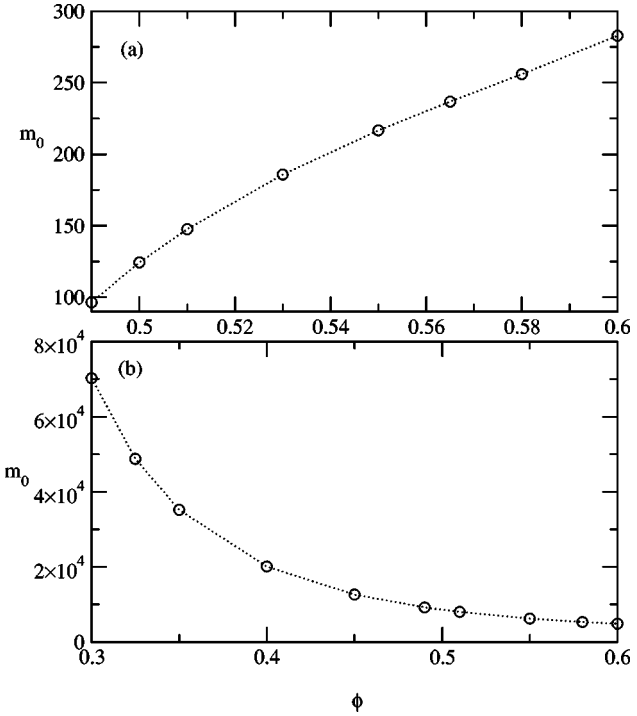


FIG. 8. (a) Longitudinal stress modulus $m_0$ as a function of the packing fraction along the isotherm $T=0.7$ . (b) Same as graph (a) but along the isotherm $T=0.3$.

## IV. CONCLUSIONS

We have studied the kinetic glass transitions of particles with a model square-well potential using mode coupling theory. This interaction potential should, we believe, be a reasonable approximation to that found in particles with grafted chains and systems with strong depletion interactions. All nontrivial results arise when the attractive piece of the interaction potential is strong, but of very short range, and we have studied a typical example of this type. Based on this, we have been able to describe some mechanical properties of two types of colloidal glasses, the one resulting mainly from attractive and the other mainly from repulsive interactions between particles. We and others [8,9,13] have earlier proposed a distinction between the two kinds of glasses based on their dynamical behavior However, in this paper we have shown that this difference may be probed experimentally using the difference in mechanical properties and that there are exponents that describe the merging of these glasses into a single glass beyond some critical density.

In general terms, glasses dominated by attractions have a stronger rigidity under shear than those originating simply from packing forces.

Also, we have studied the behavior of the zero-frequency elastic shear modulus $G'$ and the longitudinal stress modulus $m_0$ along the liquid-attractive glass transition curve. Besides being of intrinsic interest, this part of the study was chosen in the belief that comparison to experiments will be more reliable along this curve and less dependent on model potential details. The predictions are striking. This is a positive feature since even confirmation of trends will be of some interest in evaluating the MCT approach to these systems.

At lower packing fraction where we believe attractions to be completely dominant, there is a linear increase of the shear modulus with packing. This reflects the fact that also the mean number of bonds to a particle in the system is fairly linear in $\phi$ and the only relevant physical mechanism to determine the shear modulus in this region of the phase diagram occurs at short length scale. We have argued that here the shear modulus is determined by nearest-neighbor adhesions. As an aside, we note also that within MCT the attractive glass-liquid transition curve itself is essentially determined by the same factors as those determining the shear modulus.

On the contrary, at higher values of packing fraction, the shear modulus decreases quite dramatically towards typical repulsive glass values. This phenomenon originates from the changes in the nonergodicity factor that compete in Eq. (9) with those of the structure factor and lead the system to soften with respect to shear. The implication is that there should be a maximum of the shear modulus along the liquid-glass transition.

Now we turn to the longitudinal modulus of the system. Here the result is quite different from that for the shear modulus. Along the glass-liquid transition curve $m_0$ decreases with increasing density. We have observed that the transition curve passes close to the critical point and some portion of the spinodal of the underlying liquid-gas transition and consequently the input structure factor at long wavelength is very large. The prefactor in formula (11), therefore, becomes very large. The physical implication is that large scale density fluctuations quenched into the glass cause a large increase in the longitudinal modulus and the longitudinal modulus is dominated by these for much of the attractive glass regime.

We note, in passing that MCT does not always reliably predict the stability of the attractive glass. By this we mean that when we check the mean bonding number to a particle in what has been predicted to be a glass, we sometimes find that this number is even less than 2. We conclude that in these cases MCT is overemphasizing the stability of the glass, probably for a variety of reasons. In any case, we use this independent calculation as a rough check to exclude regions of MCT glass that are clearly unphysical. It will be important to address these issues in future.

There is no doubt that the model and the means by which we have studied it are simple and there are numerous limitations implied thereby. Nevertheless, the model is in some sense canonical in that it contains the essential physical input of strong short-ranged interaction and repulsion. We believe that it encompasses many essential ideas regarding the mechanical properties of colloidal glasses and we have laid these out for consideration by further theoretical, but mainly experimental researches.

## ACKNOWLEDGMENTS

We thank W. Götze and M. Fuchs for discussions and suggestions. F.S. and P.T. were supported by INFM-PRAHOP and MURST PRIN98 while E.Z., G.F. and K.A.D. were supported by INCO-Copernicus Nos. Grant IC15CT96-0756 and COST P1.

[1] J. P. Hansen and I. R. McDonald, *Theory of Simple Liquids* (Academic Press, London, 1986).
[2] W. Götze, in *Liquids, Freezing and Glass Transition*, edited by J. P. Hansen, D. Levesque, and J. Zinn-Justin (North-Holland, Amsterdam, 1991), p. 287.
[3] U. Bengtzelius, W. Gtze, and A. Sjölander, J. Phys. C **17**, 5915 (1984).
[4] E. Leutheusser, Phys. Rev. A **29**, 2765 (1984).
[5] W. van Megen, S. M. Underwood, and P. N. Pusey, Phys. Rev. Lett. **67**, 1586 (1991).
[6] W. van Megen and S. M. Underwood, Phys. Rev. Lett. **70**, 2766 (1993).
[7] W. van Megen and S. M. Underwood, Phys. Rev. Lett. **72**, 1773 (1994).
[8] J. Bergenholtz and M. Fuchs, Phys. Rev. E **59**, 5706 (1999).
[9] L. Fabbian, W. Götze, F. Sciortino, P. Tartaglia, and F. Thiery, Phys. Rev. E **59**, 1347 (1999).
[10] J. Bergenholtz and M. Fuchs, J. Phys.: Condens. Matter **11**, 10 171 (1999).
[11] J. Bergenholtz, M. Fuchs, and Th. Voigtmann, J. Phys.: Condens. Matter **12**, 6575 (2000).
[12] G. Foffi, E. Zaccarelli, F. Sciortino, P. Tartaglia and K. A. Dawson, J. Stat. Phys. **100**, 363 (2000).
[13] K. A. Dawson, G. Foffi, M. Fuchs, W. Götze, F. Sciortino, M. Sperl, P. Tartaglia, Th. Voigtmann, and E. Zaccarelli, Phys. Rev. E (to be published).
[14] H. Verduin and J. K. G. Dhont, J. Colloid Interface Sci. **172**, 425 (1995).
[15] S. M. Ilett, A. Orrock, W. C. K. Poon, and P. N. Pusey, Phys. Rev. E **51**, 1344 (1995).
[16] N. A. M. Verhaegh, D. Asnaghi, H. N. W. Lekkerkerker, M. Giglio, and L. Cipelletti, Physica A **242**, 104 (1997).
[17] L. Sjogren, J. Phys.: Condens. Matter **3**, 5023 (1991), and references therein.
[18] A. H. Scott, D. J. Scheiber, A. J. Curtis, J. I. Lauritzen, and J. D. Hoffman, J. Res. Natl. Bur. Stand., Sect. A **66**, 269 (1962).
[19] T. Nakajima and S. Saito, J. Polym. Sci. **31**, 423 (1958).
[20] F. Mallamace, P. Gambadauro, N. Micali, P. Tartaglia, C.

Liao, and S. H. Chen, Phys. Rev. Lett. **84**, 5431 (2000).
[21] T. Franosch, M. Fuchs, W. Götze, M. R. Mayr, and A. P. Singh, Phys. Rev. E **55**, 7153 (1997).
[22] W. Götze and L. Sjögren, Rep. Prog. Phys. **55**, 241 (1992); W. Götze, J. Phys.: Condens. Matter **11**, A1 (1999).
[23] G. Nagele and J. Bergenholtz, J. Chem. Phys. **108**, 9893 (1998).
[24] W. Götze and M. R. Mayr, Phys. Rev. E **61**, 587 (2000).
[25] R. J. Baxter, J. Chem. Phys. **49**, 2770 (1968).
[26] Y. C. Liu, S. H. Chen, and J. S. Huang, Phys. Rev. E **54**, 1698 (1996).
[27] M. F. Thorpe, J. Non-Cryst. Solids **57**, 355 (1984); **76**, 109 (1985).
[28] A. Rotenberg, J. Chem. Phys. **43**, 1198 (1965).